



Performance analysis of urine formed element analyzer EH-2090 was found to have good accuracy in detecting RBCs and WBCs when compared to manual microscopic

Lixia Bai[#], Qiaoping Xu[#], Zhicheng Wu

Department of Laboratory Medicine, Peking University Shenzhen Hospital, Shenzhen, China

Contributions: (I) Conception and design: Z Wu; (II) Administrative support: Z Wu; (III) Provision of study materials or patients: L Bai, Q Xu; (IV) Collection and assembly of data: L Bai, Q Xu; (V) Data analysis and interpretation: L Bai, Q Xu; (VI) Manuscript writing: All authors; (VII) Final approval of manuscript: All authors.

[#]These authors contributed equally to this work as co-first authors.

Correspondence to: Zhicheng Wu, MD. Department of Laboratory Medicine, Peking University Shenzhen Hospital, 1120 Lotus Road, Futian District, Shenzhen 518036, China. Email: wu19760702@163.com.

Background: EH-2090 is Mindray's new-generation fully automatic urine formed element analyzer (hereinafter referred to as EH-2090). Currently, there are no studies on EH-2090, so we evaluated the analytical and clinical performance of this instrument to verify that it can meet daily clinical needs, and used manual microscopy as a reference method.

Methods: The analytical performance of the EH-2090 was first evaluated for repeatability, linearity, reproducibility, and carryover. We collected urine samples from outpatient and inpatient departments of Peking University Shenzhen Hospital. Uncentrifuged urine was compared with the EH-2090 using the Fuchs–Rosenthal counting method—a quantitative reference method for microscopy—for comparative studies in terms of red blood cell (RBC) and white blood cell (WBC) counting accuracy. Passing-Bablok regression analysis was performed for RBC and WBC counts. Two laboratory technicians performed centrifugation and manual analysis (microscopy) to evaluate its performance at detecting RBCs, WBCs, and casts, sensitivities and specificities were calculated.

Results: The EH-2090's between-run reproducibility, within-day reproducibility, between-day reproducibility, and within-laboratory reproducibility for formed components of urine all met the laboratory requirements. There was a good correlation between the counting accuracy of RBCs ($r=0.965$, $P<0.0001$) and WBCs ($r=0.894$, $P<0.0001$) by the EH-2090 and the Fuchs-Rosenthal method. The positive coincidence rates of RBC and manual microscopy were 86.08% and 92.41%, respectively, and the negative coincidence rates were 88.39% and 85.81%, respectively. The positive coincidence rates before and after the WBC review were 89.33% and 92.00%, respectively, whereas the negative ones were 77.64% and 83.23%, respectively. The positive coincidence rates before and after cast review were 77.78% and 82.05%, respectively, and the negative ones were 97.09% and 93.60%, respectively.

Conclusions: The EH-2090 has good analytical and clinical performance. Its RBC and WBC counting accuracy correlates well with the quantitative reference method of microscopy.

Keywords: Urine formed element analyzer; manual microscopy; Mindray EH-2090

Submitted Dec 02, 2023. Accepted for publication Jan 25, 2024. Published online Feb 20, 2024.

doi: 10.21037/tau-23-626

View this article at: <https://dx.doi.org/10.21037/tau-23-626>

Introduction

Urine analysis is one of the most widely used analytical methods in clinical laboratories. Through urine dry-chemistry analysis, multiple physical and chemical properties of urine can be obtained at one time. Urine formed element analysis mainly includes the identification of red blood cells (RBCs), white blood cells (WBCs), casts, and other formed components in urine. Urine microscopy was introduced into clinical practice in 1830, and as microscopy technology has advanced, it has gradually become a diagnostic standard for patients with suspected kidney disease. Urine analysis may detect various diseases, such as urinary tract infection (UTI), kidney disease, and diabetes, at an early stage, and it plays a key role in evaluating acute kidney injury (AKI) (1,2). At present, the main methods for the analysis of urine formed components are manual microscopy and various types of fully automated urine analyzers. Although urine analyzers are more convenient and faster than manual microscopic examination, the examination of urine sediment by microscopy is still a reference method for urinalysis (3).

Urine formed element examination is an important part of routine urine examination. After more than 100 years of practice, it has been shown to have important diagnostic and differential-diagnostic value for kidney diseases, urinary tract diseases, and infectious diseases. Some abnormal changes that cannot be found in a general

urine test or chemical test can usually be found by the urine formed element test. Recent urine formed element analyzers operate on two main principles: digital imaging technology and flow cytometry (4). Urine analyzers based on digital image analysis use a built-in camera to capture multiple images and corresponding software for automatic component identification. In contrast, flow cytometry-based analyzers classify cellular components based on the properties of forward scattering, side scattering, and lateral fluorescence of urine sediments (5-7). Although an automated urine formed element analyzer can quickly provide the detection results of urine sediments, the subtle morphological changes and accurate identification of cellular components still must be confirmed by professional clinicians.

The Mindray EH-2090 Urine Formed Element Analyzer (Mindray, Shenzhen, China) applies computer vision imaging and recognition technology to perform morphological intelligence analysis and quantitative count detection of urine formed elements, including RBCs, WBC, WBC clumps (WBCc), bacteria (BACT), yeast (YST), squamous epithelial cells (SECs), non-squamous epithelial cells (NEC), crystals (CRYS), hyaline casts (HYAC), and unclassified casts (UNCC) in urine. "Machine vision" technology utilizes machines, sensors, and computers to simulate the eyes and hands of the laboratory professionals for measurement and judgment. When used in the analysis of urine formed elements, machine vision usually converts various urine formed elements into digital image signals through visual perception devices such as charge coupled device/complementary metal oxide semiconductor (CCD/CMOS) and image acquisition card, and transmits the digital image signals to the computer processing and analysis system. Morphological analysis of the images and image feature extraction were performed by analysis software to identify the formed elements in the urine for classification and counting.

Urine formed element detection is an important laboratory test, and the accuracy of its detection is closely related to clinical diagnosis, so accurate RBC and WBC detection is very important. And EH-2090, as the latest generation of Mindray's urine formed element analyzer, has not been evaluated in any article. At present, the commonly used conventional method is centrifugation and microscopy, so this paper uses centrifugation and microscopy as a standardized method for verification of the EH-2090. In this paper, the analytical performance of the Mindray EH-2090 was first evaluated. The Fuchs-Rosenthal counting method was used on uncentrifuged urine and the results

Highlight box

Key findings

- In this study, we validated the analytical and clinical performance of the EH-2090.

What is known and what is new?

- Urine analysis is one of the most widely used analytical methods in clinical laboratories. Urine formed element analysis mainly includes the identification of red blood cells, white blood cells, casts, and other formed components in urine.
- The Mindray EH-2090 urine formed element analyzer applies computer vision imaging and recognition technology to perform morphological intelligence analysis and quantitative count detection of urine formed elements. Its operation is simple, its degree of automation is high, and it can provide real pictures under the microscope, giving it high application value.

What is the implication, and what should change now?

- The EH-2090 provides accurate test results, providing images of the formed components of urine and reducing the workload of the laboratory technician.

were compared with those of the EH-2090 to calculate its accuracy of RBC and WBC counting. There was a good correlation between the counting accuracy of RBCs ($r=0.965$, $P<0.0001$) and WBCs ($r=0.8944$, $P<0.0001$) by the EH-2090 and the Fuchs-Rosenthal method. Then, the RBCs, WBCs, and casts were examined under the microscope after centrifugation, and the results of the abovementioned sediment components were recorded. The results were compared with those of the EH-2090 to evaluate its detection performance of RBCs, WBCs, and casts. Its RBC, WBC, and cast results have good positive coincidence rates compared to centrifugation and microscopy. We present the following article in accordance with the MDAR reporting checklist (available at <https://tau.amegroups.com/article/view/10.21037/tau-23-626/rc>).

Methods

Sample source

In this study, from January to March 2023, a total of 810 clean midstream urine samples were collected in the morning from patients in the Peking University Shenzhen Hospital Laboratory Center, including outpatients and inpatients. The samples were placed at room temperature (18–25 °C), and the detection was completed within 2 hours after collection. Sample selection and performance evaluation were based on Clinical and Laboratory Standards Institute (CLSI) GP16-A3 and EP 5-A2 (8,9). The study was approved by the Medical Ethics Committee of Peking University Shenzhen Hospital (No. 2023-174). The study was carried out in line with the Declaration of Helsinki (as revised in 2013). The obligation to collect signed informed consent from patients was waived due to the study's retrospective nature.

Instruments and reagents

The EH-2090 Urine Formed Element Analyzer (Mindray, Shenzhen, China) and accompanying quality control (Mindray, Shenzhen, China), and a Nikon microscope (Nikon, Tokyo, Japan) were used. All instruments were calibrated and well monitored for daily quality control, and all reagents were within their expiration dates.

Analytical performance verification

Reproducibility

Using Mindray I, II, III, and IV level quality control,

the 4-level quality control materials were tested twice consecutively as the first batch of test results on the same day. At intervals of at least 4 hours, the four horizontal quality control materials were continuously tested twice as the second batch of test results on the same day. The above two steps were repeated for at least 20 days. The resulting data of the quality control test were collected and used to calculate the repeatability, between-run, within-day, between-day, and within-laboratory reproducibility. Because I level quality control is a low value quality control (considered a negative sample), a result of >0 and below the RBC and WBC thresholds (RBC <10/ μ L, WBC <16/ μ L) is sufficient; II-IV level quality control RBC and WBC results should have a CV% of less than 25% at 50/ μ L and less than 15% at 200/ μ L.

Repeatability

Samples with two concentrations near the clinical cutoff value were selected for repeatability, 10 repeated tests were performed for RBC and WBC parameters, and the mean and coefficient of variation (CV%) of each sample were calculated. Among them were 17 RBC samples (sample RBC mean range 56.10–507.13) and 18 WBC samples (sample WBC mean range 66.26–753.10). RBC and WBC samples should have a CV% of less than 25% at 50/ μ L and less than 15% at 200/ μ L.

Linearity

RBC suspensions were manually prepared with concentrations of 0, 1,500, 3,000, 6,000, 12,000, 24,000, 36,000, 48,000, and 60,000/ μ L, and measured on the EH-2090 using suspensions with different concentration gradients. Each sample was tested 3 times and the average value was taken. At the theoretical concentration points of 0–60,000/ μ L, the regression equation was calculated using the theoretical concentration points as the independent variable and the measured average of each theoretical concentration point as the dependent variable. Theoretical concentrations should correlate well with the average of measured concentrations.

Carryover contamination rate

The high-value RBC and WBC samples were selected for three consecutive detections (H1, H2, H3) in comprehensive mode, and then three consecutive normal saline samples (L1, L2, L3) were detected. The carryover contamination rate was calculated according to the following formula:

$$\text{Carryover contamination rate} = \frac{L1 - L3}{H3 - L3} \times 100\% \quad [1]$$

Carryover contamination rate results should be less than 0.05%.

Reference method

Urine samples were first assayed on the EH-2090 and subsequently manually counted using Fuchs-Rosenthal chamber. Manual counts of RBCs and WBCs in urine were performed using a Fuchs-Rosenthal chamber under a phase-contrast microscope (40×), and two experienced laboratory technicians manually counted the sediment components in uncentrifuged urine under microscope. RBCs and WBCs were counted in a total of 16 large square areas of 2×3.2 μL, from which the concentrations of RBCs and WBCs in 1 μL were calculated. Among them, 76 were RBC samples and 68 were WBC samples. Using manual counting results as the gold standard. Passing-Bablok regression analysis was performed on the main parameters (RBC and WBC) for the EH-2090 and the Fuchs-Rosenthal counts. The slope and intercept of the Passing-Bablok regression were calculated within the 95% confidence interval (95% CI).

Diagnostic performance and comparison

Urine samples were first assayed on the EH-2090 than the RBCs, WBCs, and casts in the urine were centrifuged and examined by manual microscopy. A total of 10 mL of urine was placed into a special centrifuge tube and centrifuged at 400 ×g for 5 minutes. The supernatant was discarded, yielding approximately 0.2 mL of precipitate. The precipitate was resuspended in the test tube, then 20 μL of the precipitate was taken and spread evenly on a glass slide and covered by coverslips.

There were 10 high-power fields (HPFs) of view for cell component inspection and 20 low-power fields for cast inspection. All microscopic examination results were completed by two laboratory technicians, and the mean values were calculated. The thresholds for manual microscopy were 0–3/HPF for RBC counts, 0–5/HPF for WBC counts, and >1/HPF for cast counts. The thresholds for EH-2090 were 10/μL for RBC counts, 16 μL for WBC counts, and >1 μL for cast counts. And using manual microscopy results as the gold standard. From the total of 611 urine samples collected for comparison, 322 were used for comparison of RBC and WBC and 289 were used for comparison of casts. Exclusion of samples with concentrations of organic components too high to be counted, 313 samples were used for RBC comparison, 311

samples were used for WBC comparison, and 289 samples were used for cast comparison. In the comparative study, the sensitivity and specificity of RBC, WBC, and casts using centrifugation and microscopy were calculated.

Statistical analysis

Passing-Bablok regression analysis was performed on the main parameters (RBC and WBC) for the EH-2090 and the Fuchs-Rosenthal counts. The Passing-Bablok regression analysis used Analyse-it v 6.15 for statistical analysis. Comparison with manual microscopy using Kappa analysis. The Kappa analysis used GraphPad Prism 9.0.0(121) for statistical analysis.

Results

Reproducibility

The 20-day reproducibility results of continuous monitoring and testing were as follows. The repeatability, between-run, within-day, between-day, and within-laboratory reproducibility of the four concentrations of quality-control substances for RBCs and WBCs are shown in [Table S1](#). The standard deviation (SD) and CV% were in line with laboratory requirements.

Repeatability

The repeatability CV% results of each sample are shown in [Figure 1A](#). The CV% of the samples were lower than 20% when the RBC concentration was 50–100/μL, and the CV% of the samples were lower than 15% when the RBC concentration was 100–500/μL. The CV% of the samples were lower than 15% when the WBC concentration was 50–100/μL, and the CV% of the samples were lower than 20% when the WBC concentration was 100–300/μL. The reproducibility of the samples at all concentrations was below the industry standard.

Linearity

The linearity results are shown in [Figure 1B](#). The linear regression coefficients were $r > 0.99$.

Carryover contamination rate

The carryover contamination rates of RBCs and WBCs are

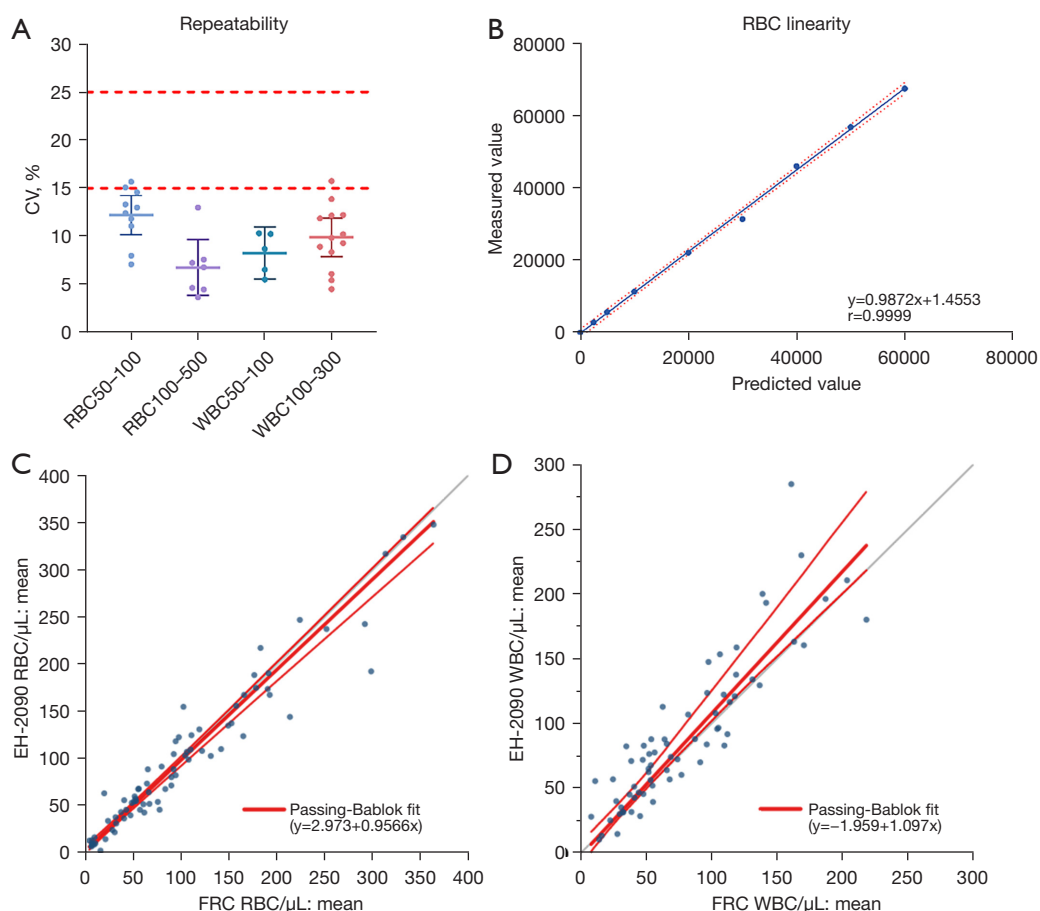


Figure 1 EH-2090 analytical performance. Repeatability (A). Linearity (B). RBC counting accuracy (C). WBC counting accuracy (D). CV, coefficient of variation; RBC, red blood cell; WBC, white blood cell; FRC, Fuchs-Rosenthal counting.

shown in Table S2. The high-value RBC and WBC samples did not carry contamination, indicating that EH-2090 has good cleaning ability and can meet the needs of clinical departments.

Comparison with the reference method

The EH-2090 detected the main parameters of RBCs and WBCs, which were compared with results of the Fuchs-Rosenthal counting. Passing-Bablok regression analysis was carried out on the results. As shown in Figure 1, since each parameter was counted in a total of 16 large square areas of $2 \times 3.2 \mu\text{L}$ and the number of manually counted cell particles was large, only samples in the range of 0–400/ μL were counted. Figure 1C compares the results of the EH-2090 RBC and Fuchs-Rosenthal method, and the regression equation was $Y=2.973+0.9566X$ ($r=0.965$, $P<0.0001$).

Figure 1D compares the results of the EH-2090 WBC and Fuchs-Rosenthal method, with the regression equation of $Y=-1.959+1.097X$ ($r=0.894$, $P<0.0001$). Both counts showed good consistency.

Diagnostic performance study

RBC test results

A total of 313 samples of urine sediments were detected by the EH-2090 and then subjected to centrifugation and manual microscopy. The two methods are compared in Table 1. Taking centrifugation and manual microscopy as the gold standard, there were 22 samples of false-negative RBCs and 18 samples false-positive RBCs after EH-2090 detection ($k=0.744$, 95% confidence interval from 0.671 to 0.818). After review by the instrument interface, there were 12 false-negative and 22 false-positive samples ($k=0.783$,

Table 1 Comparison of the EH-2090 RBC results and manual microscopy results before and after the review

Validation experiment	RBC manual microscopy results		
	Positive (abnormal)	Negative (normal)	Total
EH-2090 (before audit)			
Positive (abnormal)	136	18	154
Negative (normal)	22	137	159
Total	158	155	313
EH-2090 (after audit)			
Positive (abnormal)	146	22	168
Negative (normal)	12	133	145
Total	158	155	313

RBC, red blood cell.

Table 2 Comparison of EH-2090 WBC results and manual microscopy results before and after the review

Validation experiment	WBC manual microscopy results		
	Positive (abnormal)	Negative (normal)	Total
EH-2090 (before audit)			
Positive (abnormal)	134	36	170
Negative (normal)	16	125	141
Total	150	161	311
EH-2090 (after audit)			
Positive (abnormal)	138	27	165
Negative (normal)	12	134	146
Total	150	161	311

WBC, white blood cell.

95% confidence interval from 0.714 to 0.851) (*Table 1*).

WBC test results

A total of 311 samples of urine sediment were detected by the EH-2090 and then subjected to manual microscopy. *Table 2* compares the two methods. Taking manual microscopy as the gold standard, there were 16 samples of false-negative and 36 samples of false-positive WBCs after EH-2090 detection ($k=0.667$, 95% confidence interval from 0.585 to 0.749). After review by the instrument interface, there were 12 false-negative and 27 false-positive samples ($k=0.750$, 95% confidence interval from 0.677 to 0.823) (*Table 2*).

Cast test results

A total of 289 urine sediment samples were detected by

the EH-2090 and then subjected to manual microscopy. The results of the two methods are compared in *Table 3*. Taking manual microscopy as the gold standard, there were 26 samples of false-negative casts and 5 samples of false-positive casts after EH-2090 detection ($k=0.771$, 95% confidence interval from 0.696 to 0.846). After review by the instrument interface, there were 21 false-negative samples and 11 false-positive samples ($k=0.767$, 95% confidence interval from 0.691 to 0.843) (*Table 3*).

Positive and negative coincidence rate

The positive coincidence rates of the EH-2090 and manual microscopy are shown in *Table 4*. The positive coincidence rates before and after the RBC review were 86.08% and 92.41%, respectively; the negative rates were 88.39% and

Table 3 Comparison of the EH-2090 cast results and manual microscopy results before and after the review

Validation experiment	Cast manual microscopy results		
	Positive (abnormal)	Negative (normal)	Total
EH-2090 (before audit)			
Positive (abnormal)	91	5	96
Negative (normal)	26	167	193
Total	117	172	289
EH-2090 (after audit)			
Positive (abnormal)	96	11	107
Negative (normal)	21	161	182
Total	117	172	289

Table 4 Positive and negative coincidence rates

Coincidence rates	Preaudit RBC (%)	Post-audit RBC (%)	Preaudit WBC (%)	Post-audit WBC (%)	Preaudit cast (%)	Post-audit cast (%)
Positive consistency rate	86.08	92.41	89.33	92.00	77.78	82.05
Negative consistency rate	88.39	85.81	77.64	83.23	97.09	93.60

RBC, red blood cell; WBC, white blood cell.

85.81%. The positive coincidence rates before and after the WBC review were 89.33% and 92.00%, respectively, and the negative ones were 77.64% and 83.23%, respectively. The positive coincidence rates before and after cast review were 77.78% and 82.05%, respectively, and the negative ones were 97.09% and 93.60%, respectively.

Discussion

The automation of urine testing began in the second half of the 20th century, thanks to the development of urine dry-chemistry technology and the emergence of various types of urine dry-chemistry analysis instruments, followed by the analytical system of the morphological components of urine. Comparisons between urine formed element analyzers and manual microscopy performed by laboratory experts have shown good agreement in the identification of RBCs, WBCs, bacteria, and SEC (10-16), but the identification of renal tubular epithelial cells, transitional epithelial cells, opaque casts, and less common types of crystals has not been very accurate (4). Therefore, in actual clinical diagnosis, urine formed element analyzers without imaging capability cannot fully meet the needs of clinical practice. Most microscopes are not equipped with an integrated

digital camera, so clinicians usually cannot take pictures under the microscope. Similarly, most of the pathological images of kidney biopsy specimens are reviewed in teaching conferences, but there are few corresponding pictures of urine morphology under a microscope (17).

The urine formed element analyzer is widely used in clinical practice. The screening performance of urine testing for UTIs is widely recognized (18-21). In addition, automated urine sediment analyzers have been used to differentiate between glomerular hematuria (GH) and non-glomerular hematuria (NGH) (22). Urine testing can also be predictive of suspected uroepithelial cancer (23). Therefore, it is important that the basic performance and clinical performance of the urine formed element analyzer is accurate.

The Mindray EH-2090 is a fully automatic urine formed element analyzer with machine vision imaging and recognition technology. At the same time, it can form an assembly line with the Mindray UA-5600 dry-chemistry analyzer to conduct comprehensive testing of urine samples, which can not only assess the physical and chemical traits of the urine sample but also provide images of the sediment components present in the urine sample, which makes the urine sample information more complete, helps the

clinician to review the patient's condition, and provides reliable urine test results. However, there are no articles reporting on its basic and clinical properties. To determine whether the EH-2090 can meet the needs of clinical use, the following evaluations of its analytical performance and clinical performance were carried out in this study.

The reproducibility results are shown in [Table S1](#), and the results of the RBC and WBC measurements met the laboratory requirements. In terms of repeatability, almost all samples performed well, and the CV% of all samples did not exceed 20%, which was in line with the national industry standard. The linearity results also indicated that the EH-2090 has a wide RBC linear range ([Figure 1B](#)). The above results show that the Mindray EH-2090 urine formed element analyzer has good analytical performance. In addition, the accuracy of RBC and WBC counting was verified. The results of EH-2090 detection of RBCs and WBCs and the comparison with Fuchs-Rosenthal counting are shown in [Figure 1C,1D](#). The good agreement between the 2 indicates that EH-2090 has good RBC and WBC recognition ability and can provide accurate RBC and WBC test results.

Urine formed element detection is an important basis for diagnosing urogenital diseases and related diseases through laboratory samples, and the accuracy of its detection is closely related to clinical diagnosis. At present, the commonly used conventional method is centrifugation and microscopy, so this paper uses centrifugation and microscopy as a standardized method for verification of the EH-2090. A total of 313 urine samples were detected by the EH-2090 and then subjected to manual microscopic examination. There were 22 RBC false-negative samples without EH-2090 review, and 12 false-negative samples were found by the software review ([Table 1](#)). When we looked at the results of these 12 false-negative samples, we found that they all had few RBCs. Centrifugation and microscopy yielded 2–5 RBCs/HPF in 5 cases and 0–6 RBCs/HPF in 3 cases, accounting for approximately 60%. In these 12 samples, except for 1 case (centrifugation and microscopy result 0–6/HPF) where RBCs were not detected by the EH-2090, all RBCs were detected but did not reach the threshold. The false-positive samples were also analyzed. The 22 RBC false-negative samples were confirmed to have RBCs by the EH-2090, whereas the results of centrifugation and microscopy were mostly 0–2/HPF (10 cases) and 0–3/HPF (6 cases), respectively, where RBCs were detected. Only 1 case of RBC false negativity was detected by centrifugation and microscopy, but the

WBC result of this sample was 73–90/HP, which may have affected the RBC result.

Similarly, 311 cases of urine samples were analyzed for WBCs, with 0–5/HPF as the threshold for manual microscopy and 0–8/ μ L as the threshold for the EH-2090. There were 16 false-negative samples before review and 12 false-negative samples after review ([Table 2](#)). WBCs were detected in all false-negative samples by the EH-2090 but did not reach the threshold, whereas 27 false-positive samples were confirmed to have WBCs, and the results of centrifugation and microscopy also all showed the presence of WBCs, but none of them reached the threshold, which would not pose a significant clinical risk.

For cast counting, a total of 289 urine samples were used. The cast count >1/HPF was set as the threshold for manual microscopy, and 0–0.5/ μ L was the threshold for the EH-2090. There were 26 false-negative samples without EH-2090 review and 21 false-negative samples after review ([Table 3](#)). The microscopic examination results of these 21 false-negative samples were analyzed, and it was found that they were all samples with few casts, and the results of centrifugation and microscopy were mostly 0–2/HPF (14 cases). The false-positive samples were also analyzed. The 11 false-positive samples had cast components after EH-2090 review, whereas no casts were observed in 8 cases by centrifugation and microscopy, and the results of the other 3 cases were 0–1/HPF, which did not reach the threshold. Thus, the content of cast components was low. This type of sample needs to be given more attention.

The positive coincidence rate of the EH-2090 was higher than 80%, except for the positive coincidence rate of casts before the review. The negative concordance rates were all above 70% ([Table 4](#)). The positive concordance rates of RBCs, WBCs, and casts after the review were higher than those before the review. This is because the system misclassifies the photographed sediment components into unclassified components; these errors are corrected after review. The formed element of the samples is reclassified into the correct classification so that some samples reach the threshold, the positive samples increase, and the positive concordance rate increases.

In conclusion, the EH-2090 has a better agreement with centrifugal microscopy for RBC, WBC, and cast detection. Since the detection method adopted by the EH-2090 is to directly draw samples without centrifugation, although it has the advantages of speed, convenience, and less dosage compared with centrifugation, it will be easier to cause leakage for the sparse content of formed element. Samples

with abnormal dry chemistry and no obvious abnormalities in the organic fractions can be focused on, and such samples can be centrifuged manually for microscopic examination in order to avoid missing samples. One thing to keep in mind is that, for severe haematuria-like samples, the EH-2090 may be affected by high concentrations of RBCs leading to disturbed results for other parameters. In addition, since centrifugation is not performed, the morphology of the sediment components is not perturbed much, so it can also be used to observe the morphology of cells and casts. Furthermore, the EH-2090 has a visual image that makes it easy to review abnormal samples compared to flow cytometry analysers, which rely on manual microscopy for confirmation and increased workload due to the lack of an image. The EH-2090 provides clearer image quality than digital image technology analysers and more closely resembles the real microscopic situation.

Optical microscopy is the most commonly used method to examine urine formed element. The magnification of the microscope, the brightness adjustment, and the experience level of the examiner all affect the results. The EH-2090 can provide test results with pictures and text. It can intuitively detect the components that are prone to false-positive RBCs, such as calcium oxalate crystals, yeast, and fat globules, in clinical practice and can also detect NECs, casts, and other formed element, providing clear test results. *Figure 2* shows the detection results of the EH-2090 on some different sediment components. *Figure 2A* shows the results of some morphological RBCs, in which *Figure 2A* (a-d) show normal-morphology RBCs, which are similar in shape to RBCs in peripheral blood; *Figure 2A* (e-h) show spherical RBCs with protrusions. It can be seen that there are small spherical protrusions on the edge of the cells, of which the formation mechanism is not clear. This type of RBC can be seen in NGH. *Figure 2A* (i,j) show crenated erythrocyte, which is often formed due to dehydration of RBCs in hypertonic and acidic urine. *Figure 2A* (k,l) show RBCs with an annular shape, which are more common in glomerular diseases. *Figure 2A* (m-p) show acanthocytes, this type of RBC is more common in glomerular diseases. When such RBCs are observed, the presence of a cast should be paid attention to.

Figure 2B shows various WBCs in urine. *Figure 2B* (a-d) are neutrophils (polymorphonuclear), which are common in urinary system infections, especially acute infections such as pyelonephritis, cystitis, and urethritis. *Figure 2B* (e-h) show a mononuclear cell, which is derived from mononuclear cells in blood. When such cells appear, we should pay attention

to the test results of dry-chemistry leukocyte because the esterase in granulocytes detected by leukocyte can only detect granulocytes but not lymphocytes. Mononuclear cells may show that the dry-chemistry test results do not match the results of the sediment components. *Figure 2B* (i-l) show a deformed leukocyte, which can often be observed in cases of active inflammation such as UTI. WBC showed protruding pseudopodia and an amoeba-like shape, which is common in stained specimens but rare in S-stained specimens. *Figure 2B* (m-o) show phagocytic cells, which are commonly found in UTIs, glomerulonephritis, and IgA nephropathy.

Epithelial cells are shown in *Figure 2C*. *Figure 2C* (a-c) show SECs. A few SECs can be seen in the urine of healthy people. Many SECs with increased WBCs often indicate urethritis. *Figure 2C* (d-f) show the superficial urothelium. *Figure 2C* (g-i) show the underlying urothelium, and the appearance of different parts of the epithelium indicates lesions in the corresponding parts. *Figure 2C* (j-l) show a decoy cell, which is a shed renal tubular epithelial cell containing polyoma viral inclusion bodies, which are related to BKV (BK virus) infection and renal insufficiency after renal transplantation (24-26).

Figure 2D shows the hyaline cast, which can appear in large numbers in malignant hypertension, acute and chronic glomerulonephritis, nephrotic syndrome, etc. *Figure 2E* shows the cellular cast, which can be divided into three types depending on the cells contained within the cast: erythrocyte casts, leukocyte casts, and tubular epithelial cell casts. They also have different clinical significance. Granular casts, as shown in *Figure 2F*, often indicate substantial renal lesions, whereas waxy casts (*Figure 2G*) indicate severe tubular necrosis or chronic damage to nephrons, which are more common in advanced chronic glomerulonephritis and chronic renal failure. There is a theory that the casts formed in the renal tubules will degenerate and deteriorate and gradually form coarse-grained casts or fine-grained casts when they stay in the kidney for too long and will further evolve to a waxy cast in the case of long-term anuria or oliguria. Different urine sediments have different clinical significance, so clear sediment results can help clinicians make diagnoses. In addition to the abovementioned sediments, the EH-2090 can distinguish various common crystals, which can not only meet daily clinical work requirements but also be used for teaching.

Conclusions

EH-2090 has good analytical performance. Its RBC,

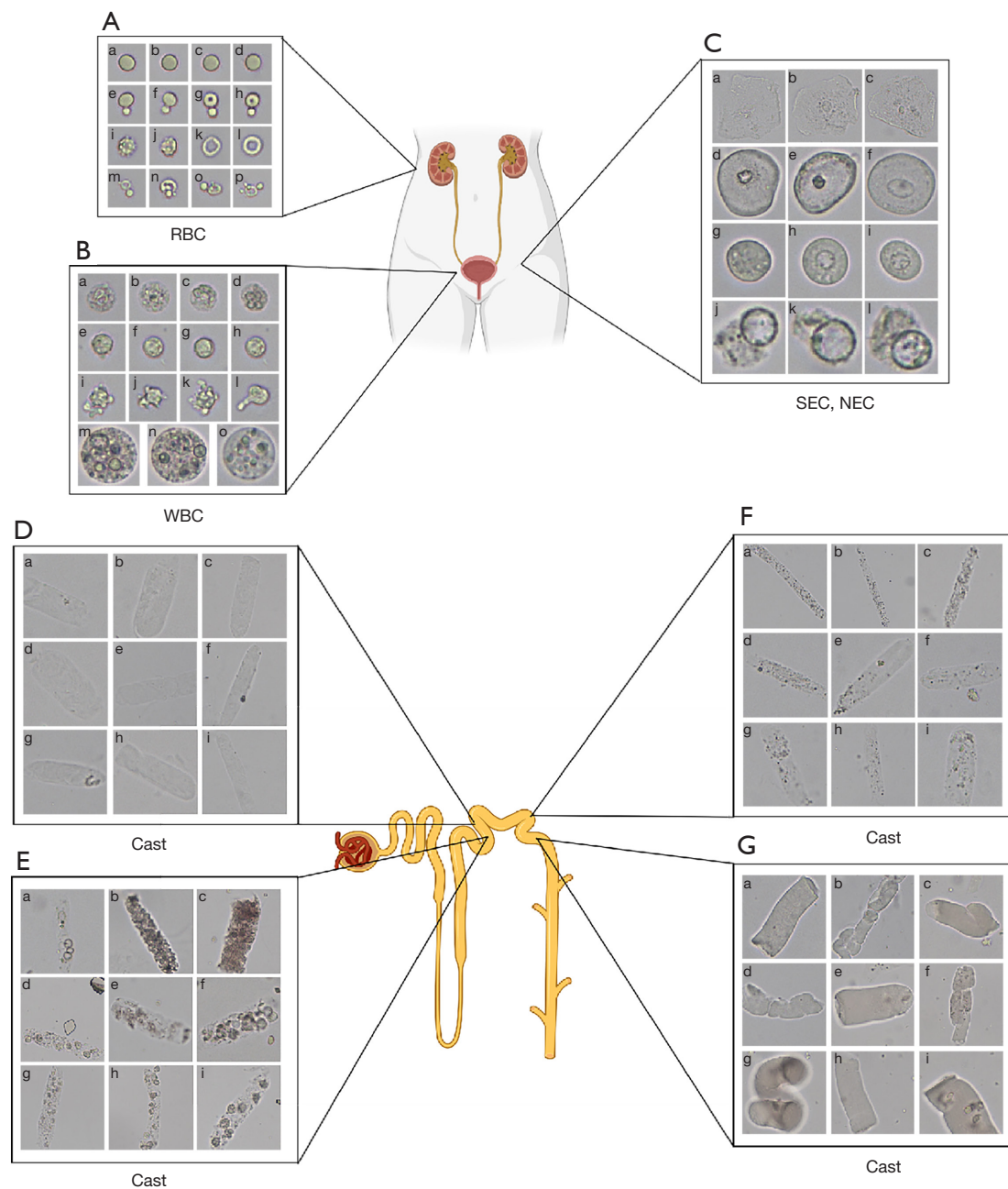


Figure 2 The human body schema was adapted from BioRender.com [2023] and permission for publication has been obtained. EH-2090 image. (A) Various forms of RBCs; (B) various forms of WBCs; (C) SEC and NEC; (D) hyaline cast; (E) cellular cast; (F) granular casts; (G) waxy casts. RBC, red blood cells; WBC, white blood cell; SEC, squamous epithelial cell; NEC, non-squamous epithelial cell. (Created with BioRender.com)

WBC, and cast results have good positive coincidence rates compared to centrifugation and microscopy. Its operation is simple, its degree of automation is high, and it can provide real pictures under the microscope, giving

it high clinical application value. Since the samples are not concentrated by centrifugation, some rare sediment components and the contingency of the observation area may cause some components to be missed. Extra attention

should be paid to samples with abnormal dry-chemistry and no obvious abnormalities in the sediments to avoid missed inspection.

Acknowledgments

Funding: This study was funded by the Wu Jieping Medical Foundation Clinical Research Special Grant Fund (No. 320.6750.2022-06-21).

Footnote

Reporting Checklist: The authors have completed the MDAR reporting checklist. Available at <https://tau.amegroups.com/article/view/10.21037/tau-23-626/rc>

Data Sharing Statement: Available at <https://tau.amegroups.com/article/view/10.21037/tau-23-626/dss>

Peer Review File: Available at <https://tau.amegroups.com/article/view/10.21037/tau-23-626/prf>

Conflicts of Interest: All authors have completed the ICMJE uniform disclosure form (available at <https://tau.amegroups.com/article/view/10.21037/tau-23-626/coif>). The authors have no conflicts of interest to declare.

Ethical Statement: The authors are accountable for all aspects of the work in ensuring that questions related to the accuracy or integrity of any part of the work are appropriately investigated and resolved. The study was approved by the Medical Ethics Committee of Peking University Shenzhen Hospital (No. 2023-174). The study was carried out in line with the Declaration of Helsinki (as revised in 2013). The obligation to collect signed informed consent from patients was waived due to the study's retrospective nature.

Open Access Statement: This is an Open Access article distributed in accordance with the Creative Commons Attribution-NonCommercial-NoDerivs 4.0 International License (CC BY-NC-ND 4.0), which permits the non-commercial replication and distribution of the article with the strict proviso that no changes or edits are made and the original work is properly cited (including links to both the formal publication through the relevant DOI and the license). See: <https://creativecommons.org/licenses/by-nc-nd/4.0/>.

References

1. Enko D, Stelzer I, Böckl M, et al. Comparison of the diagnostic performance of two automated urine sediment analyzers with manual phase-contrast microscopy. *Clin Chem Lab Med* 2020;58:268-73.
2. Perazella MA. The urine sediment as a biomarker of kidney disease. *Am J Kidney Dis* 2015;66:748-55.
3. Verdesca S, Brambilla C, Garigali G, et al. How a skillful (correction of skilful) and motivated urinary sediment examination can save the kidneys. *Nephrol Dial Transplant* 2007;22:1778-81.
4. Becker GJ, Garigali G, Fogazzi GB. Advances in Urine Microscopy. *Am J Kidney Dis* 2016;67:954-64.
5. Altekin E, Kadiçesme O, Akan P, et al. New generation IQ-200 automated urine microscopy analyzer compared with KOVA cell chamber. *J Clin Lab Anal* 2010;24:67-71.
6. Delanghe JR, Kouri TT, Huber AR, et al. The role of automated urine particle flow cytometry in clinical practice. *Clin Chim Acta* 2000;301:1-18.
7. Cho J, Oh KJ, Jeon BC, et al. Comparison of five automated urine sediment analyzers with manual microscopy for accurate identification of urine sediment. *Clin Chem Lab Med* 2019;57:1744-53.
8. CLSI GP16-A3: Urinalysis; Approved Guideline - Third Edition. 2009. Available online: <https://clsi.org>
9. CLSI EP5-A2: Evaluation of Precision Performance of Clinical Chemistry Devices. Approved Guideline-Second Edition. 2004. Available online: <http://clsi.org>
10. Akin OK, Serdar MA, Cizmeci Z, et al. Comparison of LabUMat-with-UriSed and iQ200 fully automatic urine sediment analysers with manual urine analysis. *Biotechnol Appl Biochem* 2009;53:139-44.
11. Zaman Z, Fogazzi GB, Garigali G, et al. Urine sediment analysis: Analytical and diagnostic performance of sediMAX - a new automated microscopy image-based urine sediment analyser. *Clin Chim Acta* 2010;411:147-54.
12. Kucukgergin C, Ademoglu E, Omer B, et al. Performance of automated urine analyzers using flow cytometric and digital image-based technology in routine urinalysis. *Scand J Clin Lab Invest* 2019;79:468-74.
13. Boven LA, Kemperman H, Demir A. A comparative analysis of the Iris iQ200 with manual microscopy as a diagnostic tool for dysmorphic erythrocytes in urine. *Clin Chem Lab Med* 2012;50:751-3.
14. Budak YU, Huysal K. Comparison of three automated systems for urine chemistry and sediment analysis in routine laboratory practice. *Clin Lab* 2011;57:47-52.

15. Ma J, Wang C, Yue J, et al. Clinical laboratory urine analysis: comparison of the UriSed automated microscopic analyzer and the manual microscopy. *Clin Lab* 2013;59:1297-303.
16. Bottini PV, Martinez MH, Garlipp CR. Urinalysis: comparison between microscopic analysis and a new automated microscopy image-based urine sediment instrument. *Clin Lab* 2014;60:693-7.
17. Mutter WP, Brown RS. Point-of-care photomicroscopy of urine. *N Engl J Med* 2011;364:1880-1.
18. Wang H, Han FF, Wen JX, et al. Accuracy of the Sysmex UF-5000 analyzer for urinary tract infection screening and pathogen classification. *PLoS One* 2023;18:e0281118.
19. Chun TT, Ruan X, Ng SL, et al. The diagnostic value of rapid urine test platform UF-5000 for suspected urinary tract infection at the emergency department. *Front Cell Infect Microbiol* 2022;12:936854.
20. Szmulik M, Trzeźniewska-Ofiara Z, Mendrycka M, et al. A novel approach to screening and managing the urinary tract infections suspected sample in the general human population. *Front Cell Infect Microbiol* 2022;12:915288.
21. Chen Y, Zhang Z, Diao Y, et al. Combination of UC-3500 and UF-5000 as a quick and effective method to exclude bacterial urinary tract infection. *J Infect Chemother* 2023;29:667-72.
22. Cho H, Yoo J, Kim H, et al. Diagnostic Characteristics of Urinary Red Blood Cell Distribution Incorporated in UF-5000 for Differentiation of Glomerular and Non-Glomerular Hematuria. *Ann Lab Med* 2022;42:160-8.
23. Ren C, Wang X, Yang C, et al. Investigation of Atyp.C using UF-5000 flow cytometer in patients with a suspected diagnosis of urothelial carcinoma: a single-center study. *Diagn Pathol* 2020;15:77.
24. Tummidi S, Kothari K, Agnihotri M, et al. Diagnostic utility of urine cytology in detection of decoy cells in renal transplant patients: Report of five cases and review of literature. *Diagn Cytopathol* 2020;48:222-7.
25. Funahashi Y, Kato M, Fujita T, et al. Association Between the Polyomaviruses Titers and Decoy Cell Positivity Rates After Renal Transplantation. *Transplant Proc* 2016;48:921-3.
26. Koh MJ, Lim BJ, Noh S, et al. Urinary decoy cell grading and its clinical implications. *Korean J Pathol* 2012;46:233-6.

Cite this article as: Bai L, Xu Q, Wu Z. Performance analysis of urine formed element analyzer EH-2090 was found to have good accuracy in detecting RBCs and WBCs when compared to manual microscopic. *Transl Androl Urol* 2024;13(2):218-229. doi: 10.21037/tau-23-626

Supplementary

Table S1 Reproducibility results

Parameters	Control level	N	Mean	Repeatability		Between-run		Within-day		Between-day		Within-laboratory	
				SD	CV%	SD	CV%	SD	CV%	SD	CV%	SD	CV%
RBC	Level 1	20	4.17	1.62	39.0%	0.00	0.0%	1.62	39.0%	0.00	0.0%	1.62	39.0%
	Level 2	20	47.94	5.12	10.7%	2.46	5.1%	5.68	11.8%	0.00	0.0%	5.68	11.8%
	Level 3	20	219.65	11.08	5.0%	0.00	0.0%	11.08	5.0%	4.55	2.1%	11.98	5.5%
	Level 4	20	990.77	29.70	3.0%	13.93	1.4%	32.81	3.3%	18.43	1.9%	37.63	3.8%
WBC	Level 1	20	4.33	1.40	32.3%	0.37	8.6%	1.45	33.4%	0.25	5.7%	1.47	33.9%
	Level 2	20	49.83	4.47	9.0%	0.94	1.9%	4.56	9.2%	2.77	5.6%	5.34	10.7%
	Level 3	20	227.47	14.18	6.2%	3.41	1.5%	14.58	6.4%	2.30	1.0%	14.76	6.5%
	Level 4	20	1,144.10	36.03	3.1%	20.34	1.8%	41.37	3.6%	14.75	1.3%	43.92	3.8%

RBC, red blood cells; WBC, white blood cells; SD, standard deviation; CV, coefficient of variation.

Table S2 Results of carryover rate

Parameters	Level	Sample 1	Sample 2	Sample 3	Sample 4	Sample 5	Sample 6	Sample 7	Sample 8	Sample 9	Sample 10
RBC	H1	3,265.00	3,468.00	4,468.10	4,485.90	5,215.00	5,493.70	10,430.40	11,055.90	77,804.20	87,118.90
	H2	3,105.00	3,637.80	4,438.70	4,441.00	5,256.60	5,657.80	10,510.80	12,080.10	84,846.10	80,979.00
	H3	3,011.00	3,462.00	4,627.70	4,279.70	5,392.50	5,375.00	10,669.70	11,305.60	85,293.70	74,454.50
	L1	0.00	0.00	0.50	0.00	0.50	0.50	0.50	0.00	1.00	2.80
	L2	0.00	0.00	0.00	0.00	0.50	0.50	0.00	0.00	0.50	1.40
	L3	0.00	0.00	0.00	0.00	0.00	0.00	0.00	0.00	0.00	0.00
	Carryover	0.00%	0.00%	0.01%	0.00%	0.01%	0.01%	0.00%	0.00%	0.00%	0.00%
WBC	H1	3,763.90	4,054.50	4,900.40	5,807.30	6,062.90	6,625.10	8,643.40	8,710.70	10,682.00	10,990.20
	H2	4,004.60	4,526.80	5,057.50	6,148.30	6,562.40	6,714.40	8,615.40	9,495.80	10,832.00	10,275.90
	H3	3,727.70	3,522.90	5,124.80	5,868.10	6,180.30	6,620.80	8,053.10	8,228.90	11,065.00	9,830.30
	L1	1.40	0.50	0.90	0.50	0.00	0.90	0.50	0.50	0.00	0.90
	L2	0.00	0.00	0.00	0.00	0.00	0.00	0.00	0.00	0.00	0.00
	L3	0.00	0.00	0.50	0.50	0.00	0.00	0.00	0.50	0.00	0.50
	Carryover	0.04%	0.01%	0.01%	0.00%	0.00%	0.01%	0.01%	0.00%	0.00%	0.00%

RBC, red blood cell; WBC, white blood cell.